Journal of the Korean Society of Marine Engineering, Vol. 38, No. 8 pp. 974~980, 2014
J. Korean Soc. of Marine Engineering (JKOSME)
http://dx.doi.org/10.5916/jkosme.2014.38.8.974

ISSN 2234-7925 (Print)
ISSN 2234-8352 (Online)
Original Paper

Effects of rotation speed and time in potentiostatic experiment in seawater for 5083-H116 Al alloy

Seung-Jun Lee[1]· Min-Su Han[2]· Seok-Ki Jang[3]· Seong-Jong Kim[†]

(Received June 20, 2014 ; Revised October 14, 2014 ; Accepted October 30, 2014)

Abstract: Aluminum acts as sacrificial anode and corrosion protection with Al_2O_3 formation. If the same current on material for Al ships with steel ships supplies, the more hydrogen would be occurred, that result is bring about over-protection. For this reason, the damage by hydrogen embrittlement leads to the serious accident. In this study, we evaluate electrochemical behavior with rotation speed of 5083-H116 Al alloy material for Al ship in seawater. To examine the electrochemical characteristics with rotation speed and its effects on performance, experiments were conducted at four rotation speed. Results of experiments, the corrosion current density and damage were increased by applying the rotation speed compared to static state.

Keywords: Al alloy, Rotation speed, Corrosion, Potentiostatic experiment, Seawater

1. Introduction

Al alloy has advantages over steel in that it has low specific gravity and high specific strength, excellent machinability and corrosion resistance, and its mechanical properties do not degrade at low temperatures. Thus, Al alloy is widely used as a light-weight material for aircrafts, automobiles, railroad cars, and ships. Furthermore, the use of high-strength Al alloy in special ships is gradually increasing. The specific rigidity of Al alloy is almost identical to that of steel, but its specific strength is almost twice as high as that of the steel. When a ship is manufactured with Al alloy in accordance with design standards, the ship weight is about 1/3 of the steel ship **[1]**. In particular, the 5083 series is widely used as a material for ship structures because it not only has all the unique advantages of Al, but also has excellent machinability and weldability. Many studies have been conducted on the electrochemical corrosion and corrosion resistance characteristics in welding conditions (e.g., friction stir welding, TIG welding, MIG welding) and seawater environment on various materials for Al ships **[2]-[4]**. This study observed the electrochemical behaviors of the 5083-H116 Al alloy which is a ship material with applied potential and rotation speed.

2. Experimental procedure

The 5083-H116 Al alloy used in the present experiments was made by adding 4.74% Mg with Mn, Si, and Cr as very small amount elements to increase its strength and ductility (**Table 1**). It was adopted in this study because as a non-heat-treated alloy it is widely used in welding structures such as ships, vehicles, and marine plants due to its superior strength and weldability. To examine the electrochemical characteristics with rotation speed by using agitator and its effects on performance, experiments were conducted at four rotation speed variables using static state. For the potentiostatic electrochemical experiment specimens, an area of 1cm^2 was exposed and mounted with epoxy. Before experiment, they were polished with an emery paper #2000, cleaned with ethanol and distilled water, and dried. The potentiostatic experiment was conducted for 1,200 s and 3600 s at a constant potential to evaluate the corrosion characteristics with applied potential in seawater. The reference electrode and counter electrode were Ag/AgCl

Table 1: Chemical compositions of 5083-H116 Al alloy (mass fraction, %)

Fe	Mn	Si	Cu	Cr	Mg	Ti	Zn	Al
0.25	0.72	0.11	0.08	0.09	4.74	0.01	0.13	Bal.

† Corresponding Author (ORCID: http://orcid.org/0000-0002-6356-3818): Division of Marine Engineering, Mokpo Maritime University, Mokpo 530-729, Korea, E-mail: ksj@mmu.ac.kr, Tel: 061-240-7226
1 Division of Marine Engineering, Mokpo Maritime University, E-mail: corr-pro@mmu.ac.kr, Tel: 010-4501-6530
2 Division of Marine Engineering, Mokpo Maritime University, E-mail: mp949@mmu.ac.kr, Tel: 061-240-7230
3 Division of Marine Engineering, Mokpo Maritime University, E-mail: skjang@mmu.ac.kr, Tel: 061-240-7205

electrode and Pt electrode, respectively. For microscopic analysis and evaluation after experiment, the corrosion pattern of the surface was observed with a 3D microscope.

3. Experimental results and discussion

Figure 1 shows a graph of the time-current density curve from a potentiostatic experiment with rotation speed which was performed for 3,600 seconds to identify the corrosion tendency at various potentials. At the applied potential of -1.9 V, it showed a very high current density of over 10^{-2} A/cm^2, but no clear difference by changing rotation speed was observed. This was a very severe condition that could cause hydrogen embrittlement. The reason for this result appears to be that the effect of the applied potential was dominant compared to the electrochemical effect resulting from the flow. At -1.5 V, it increased in a step pattern at all conditions. The reason for this appears to be that corrosion developed simultaneously with immersion and the current density maintained a constant value as a passive film was formed **[5][6]**. The highest current density reached its peak between 900 and 1,600 seconds and then steadily decreased until the end of the experiment. The reason for this appears to be that a passive film was formed by adequate oxygen supply with flow at all conditions. Furthermore, since the diffusion layer becomes thinner when there is flow, a decrease of this diffusion layer put the material in a more active state and brought about a higher current density than in static condition **[7]**. At -1.2 V, the current density gradually increased until the end of the experiment, and the current density was the lowest in static condition. The current density varied greatly depending on the existence of flow. At -0.6 V, all specimens maintained constant current density values during the experiment. However, they showed the highest current density in static condition and the lowest current density values at 400 rpm. At higher rotation speed, current density increases because the interaction between Al alloy surface and solution increases. The corrosion matters and dissolved metal ions are actively removed. At this potential, however, the supply of dissolved oxygen became active with increasing rotation speed which facilitated the formation of a passive film and lowered the current density value.

Figure 2 depicts a graph of current density values of the 5083-H116 Al alloy after potentiostatic experiment with rotation speed for 3,600 seconds. Overall, it maintained lower current density values in static condition compared to when there was flow. At specific potentials (-0.65 V, -1.7

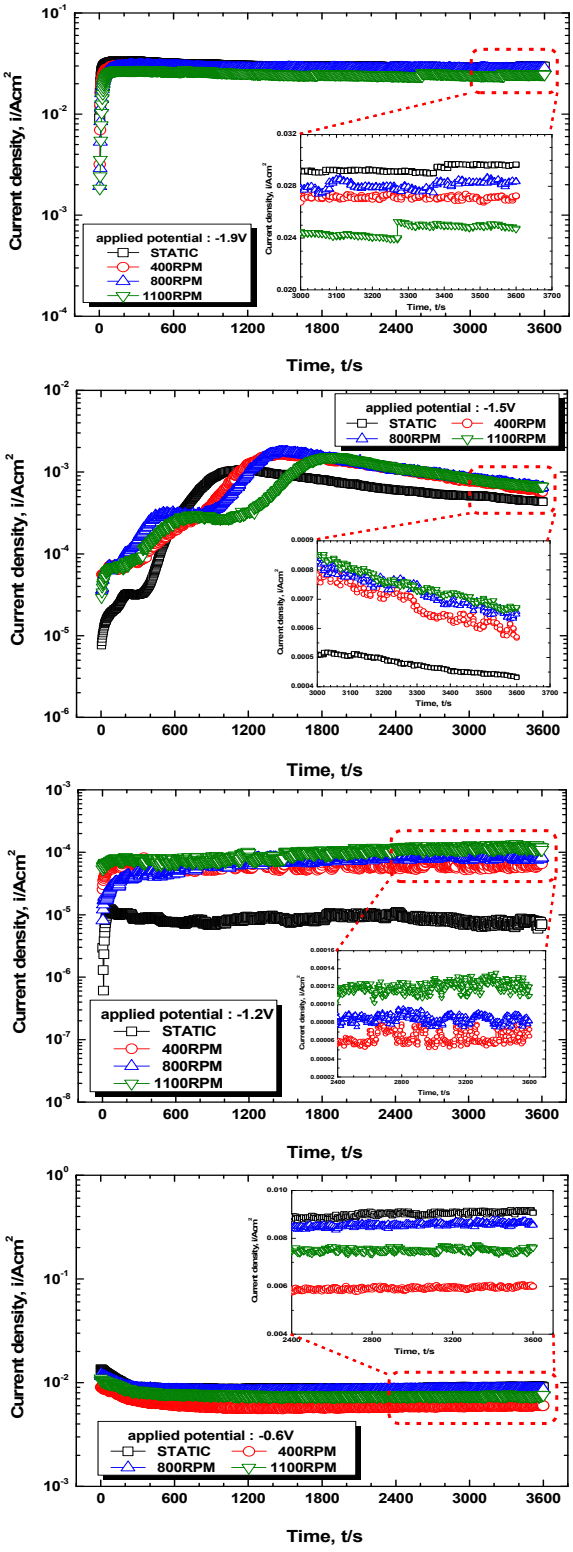

Figure 1: Time-current density curves in potentiostatic experiment with rotation speed for 5083-H116 Al alloy

V), however, the current density values reversed because oxygen supply increased by flow and this facilitated the formation of a passive film. The current density was the lowest at -0.9 V, which appears to be caused by concentration

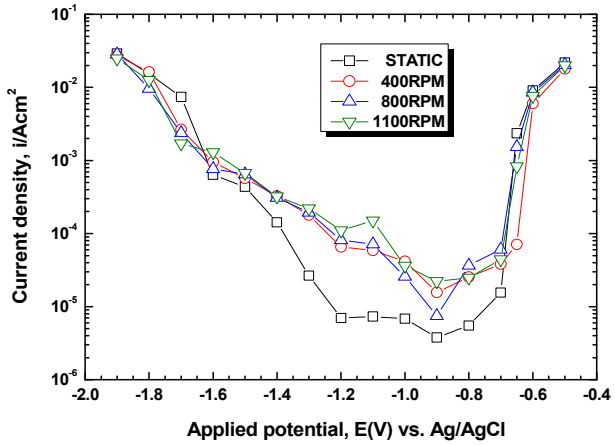

Figure 2: Comparison of current density after potentiostatic experiment for 3,600sec. with rotation speed of 5083-H116 Al alloy

polarization with dissolved oxygen reduction reaction due to the potential that is close to the open circuit potential. Particularly, in the corrosion resistance section, the current density values varied greatly by the existence of flow. The reason for this appears to be that the rotation speed increased the interaction between metal surface and solution, and promoted the removal of corrosion matters and dissolved metal ions **[8]**. Furthermore, the current density values were partially higher at low rpm because although oxygen supply to the solution increased with the increasing rotation speed, the vortex created by excessive rotation speed generated air bubbles which decreased the effective area required for the interaction between solution and metals.

Figure 3 presents the surface morphologies of the 5083-H116 Al alloy taken with a 3D microscope after

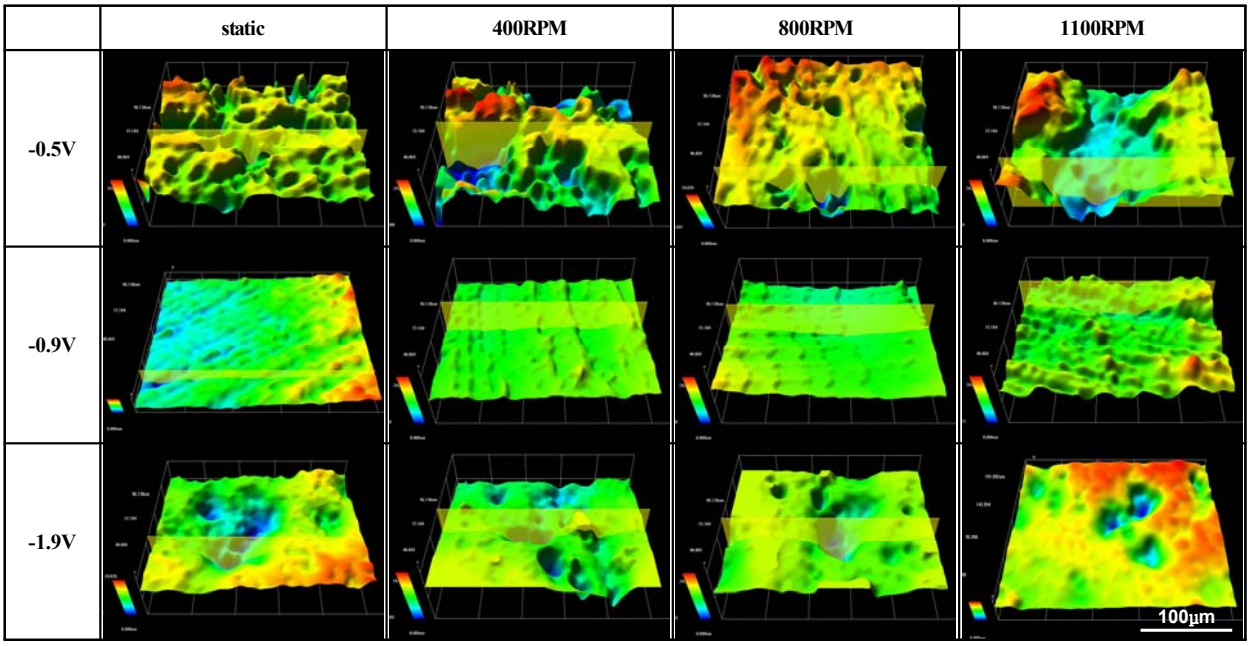

(a) Surface morphologies

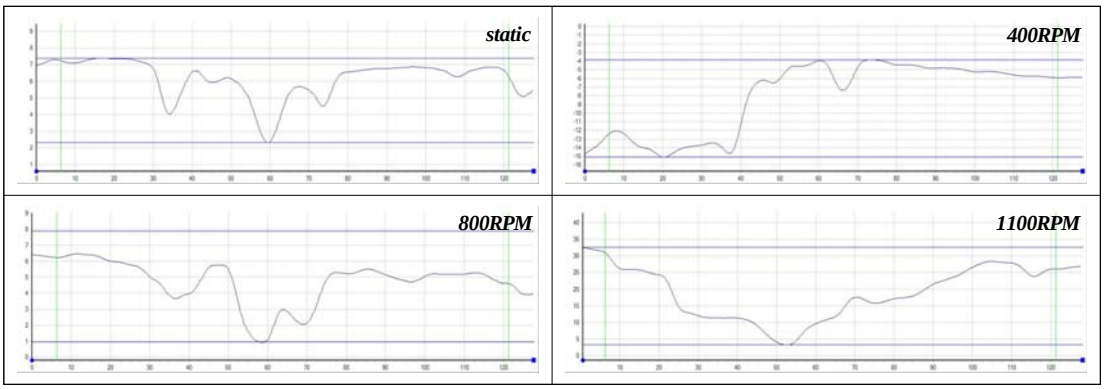

(b) Line profile at -0.5 V

Figure 3: 3D analysis after potentiostatic experiment of 5083-H116 Al alloy with rotation speed

potentiostatic experiment for 3,600 s at different rotation speed. At the applied potential of -0.5 V, in static condition, severe damages resulting from excessively active dissolution reaction were observed. When a rotation speed was applied, however, the surface became flat due to physical erosion and the damages concentrated at the center of the specimen. During the potentiostatic experiment, the current density was high at all conditions and no big difference was observed. The damages were the smallest in static condition and at 800 rpm, the greatest at 1,100 rpm. At 400 rpm, damages were mainly caused by dissolution reaction due to low rotation speed and high current density. At 1,100 rpm, the damages were the greatest due to high current density and active erosion. On the other hand, at 800 rpm, the surface was relatively clean and damages were small because the damaging actions were offset as proper flow and current were supplied. Thus, at this potential, physical erosion had greater effect than corrosion by electrochemical reaction. At the applied potential of -0.9 V, which is close to the open circuit potential and corresponds to the corrosion resistance region, the surface geometry was good in general regardless of the existence of flow. A comparison of current density after the potentiostatic experiment found that although there were differences in rotation speed, the degree of damages was insignificant as it corresponded to the corrosion resistance region. The potentiostatic experiment results in **Figure 2** showed that damages increased along with the rotation speed even at low current density values, but there were no significant differences at this potential. Thus, the specimens could be damaged not only by flow but also by electrochemical reaction. At the applied potential of -1.9 V, the highest current density value was reached during the potentiostatic experiment, and severe damages were observed due to the activation reaction by hydrogen gas in all sections regardless of rotation speed. The current density values were compared after the potentiostatic experiment and they showed almost identical values. As the rotation speed increased, however, flow was generated simultaneously with physical erosion under severe electrochemical conditions, which caused more significant damages than in static condition **[9]**.

Figure 4 compared the maximum damage depth and mean damage depth of the 5083-H116 Al alloy which were measured through 'Dynamic Eye Real' program of 3D analysis microscope after the potentiostatic experiment at different rotation speed. At the applied potential of -0.65 V, in static condition, the maximum and mean damage depths were 3.3 ㎛ and 1.2 ㎛, respectively. Damages are fewer at

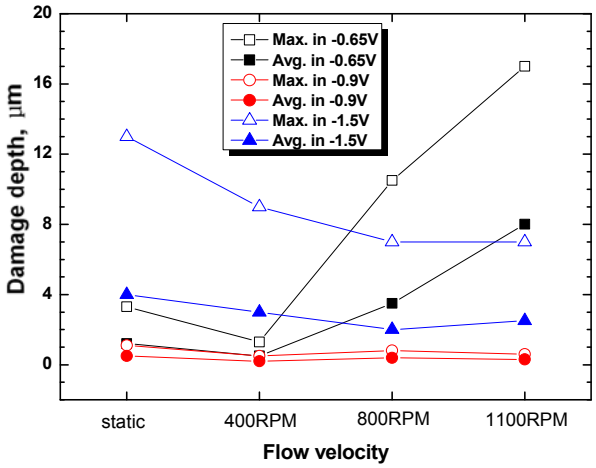

Figure 4: Comparison of damage depth after potentiostatic experiment with applied potential and rotation speed of 5083-H116 Al alloy

400 rpm than in static condition is because at 400 rpm, current density is low due to low rotation speed than other rotation speed conditions as shown in the potentiostatic experiment results. The reason that damages are greater at 800 and 1,100 rpm compared to static condition even at lower current densities appears to be that the erosion of solution was more dominant than the electrochemical reaction. Consequently, we can see that the combination of electrochemical reaction and physical erosion caused the damages of the specimen. At the applied potential of -0.9 V, in static condition, the maximum and mean damage depths were 1.1 ㎛ and 0.5 ㎛. As this corresponded to corrosion resistance potential, there was no damage by corrosion. Furthermore, the difference was very small, so damage depth by rotation speed is not very meaningful. At the applied potential of -1.5 V, in static condition, the maximum and mean damage depths were 13 ㎛ and 4 ㎛, respectively. At 400, 800, and 1,100 rpms, the maximum damage depths were 9 ㎛, 7 ㎛, and 7 ㎛, respectively, and the mean damage depths were 3 ㎛, 2 ㎛, and 2.5 ㎛, respectively. Unlike other conditions, the mean damage depths were smaller compared to maximum damage depths because local damages occurred in the depth direction due to activation by dissolution reaction and the generation of hydrogen gas. It seems that the effect of electrochemical reaction is more dominant than the effect of flow. This appears to be due the buffer effect resulting from the collision of the flow formed by the generation of hydrogen gas with the flow of the fluid. Thus, even though damages can occur by the generation of hydrogen gas, a high rotation speed may decrease physical erosion to some

degree.

Figure 5 shows a graph of current density values of the 5083-H116 Al alloy after potentiostatic experiment for 1,200 and 3,600 seconds. As a result of experiments for 1,200 seconds at -0.75 V, the current density was the lowest at 1.18×10^{-6}A/cm^2, which appears to be caused by concentration polarization with dissolved oxygen reduction reaction due to the potential that is close to the open circuit potential. At the potential of -0.7 V, the current density greatly increased compared to -0.75 V, and it also increased greatly along with rising potential at -0.7 ~ -0.5 V. It is expected that the passive film will be destroyed by excessive active dissolution reaction due to the chlorine ions in seawater solution and stress corrosion cracking will appear when there is an external stress. At -1.5 ~ -1.3 V, the current density gradually increased as the potential moved toward the active direction due to the effect of atomic hydrogen. The potential between -1.3 ~ -1.25 V corresponds to corrosion resistance section and activation response section, and the active potential was associated with higher current density, because the effect of molecule hydrogen was greater than the effect of atomic hydrogen. At the experiment time of 3,600 seconds, the mean current density at -0.8 V was the lowest at 3.779×10^{-6} A/cm^2. At the potential of -0.65 V, the current density greatly increased compared to -0.7 V, and it also increased greatly along with rising potential at -0.65 ~ -0.5 V. At -1.6 ~ -1.3 V, the current density gradually increased as the potential moved toward the active direction due to the effect of atomic hydrogen. The potential of -1.3 V corresponds to corrosion resistance section and activation response section, and the current density was somewhat low due to the dominant effect of atomic hydrogen. Furthermore, at -1.9 ~ -1.7 V, the more active the potential was, the higher the current density became due to the effect of molecule hydrogen. In general, the case of -1.9 V would generate the greatest damages because it showed the highest current density and the case of -0.9 V would generate the smallest damages because it showed the lowest current density.

Figure 6 shows a graph comparing the maximum damage depth and mean damage depth of the 5083-H116 Al alloy determined from a 3D surface analysis after the potentiostatic experiment. At the 1,200 seconds of experiment time, the curve was similar to the time-current density curve of the potentiostatic experiment. In the corrosion resistance section of -1.25 ~ -0.75 V and the activation polarization section, the smallest damages were observed at the potentials of -1.5 V and -1.4 V which were under the effect of atomic hydrogen. The damages were the severest at -0.5 V when the active dissolution reaction occurred, and at -1.8 V which was under the effect of atomic hydrogen. Even though the current density values were similar, the surface damage was severer at -0.5 V. In the case of potentiostatic experiment for 3,600 seconds, in the corrosion resistance section of -1.2 ~ -0.8 V and the activation polarization section, the damages were the smallest at -1.4 V which was under the effect of atomic hydrogen. The damages were the severest at -0.5 V when the active dissolution reaction occurred and at -1.8 V which was under the effect of atomic hydrogen. Even though the current density values were similar, the surface damage was severer at -1.8 V. Furthermore, the mean damage depth decreased at

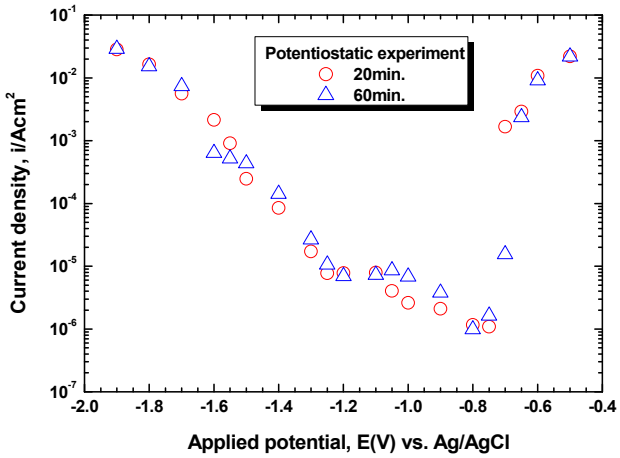

Figure 5: Comparison of current density after potentiostatic experiment during 1,200 sec. and 3,600 sec. for 5083-H116 Al alloy

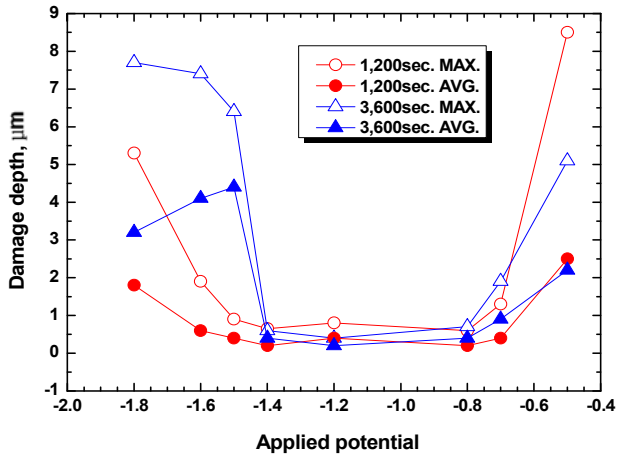

Figure 6: Comparison of damage depth after potentiostatic experiment of 5083-H116 Al alloy

-1.7 V and -1.8 V because the damage in the depth direction seemed small as the damaged parts were combined and widened due to the effect of molecular hydrogen. At all conditions, the section from -1.4 V to -0.8 V seems to be the corrosion resistance section with the smallest damages based on damage depth. In this section, the damages were extremely small with the maximum and mean damage depths under 1 ㎛ regardless of the experiment time and applied potential. Hydrogen gas generation section under -1.5 V and the active dissolution reaction section above -0.7 V were excessive damages occurred. Furthermore, considering that there was no difference by potentiostatic experiment time in the corrosion resistance section, it is expected that this corrosion resistance range will not be exceeded even after long-term operation in a ship.

Figure 7 presents surface morphologies over time of the 5083-H116 Al alloy for ship after the potentiostatic experiment. In the case of 1,200 seconds of experiment time, severe corrosion and rough surface morphologies were observed at -0.5 V due to high current density resulting from active dissolution reaction, and the 3D analysis found that the maximum damage depth and the mean damage depth were 8.5 ㎛ and 2.5 ㎛, respectively. At -0.8 V, which corresponded to the corrosion resistance section on the current density curve, both specimens showed clear surface morphology with almost no corrosion. In this condition, the maximum damage depth and the mean damage depth were 0.6 ㎛ and 0.2 ㎛, respectively, but it appears that they were just scratches during the polishing of the specimens and no damages occurred by corrosion. At -1.6 V and -1.8 V, as the potential moved to the active direction, damages became severe due to the activation polarization resulting from the generation of hydrogen gas. The maximum damage depth and the mean damage depth were 1.9 ㎛ and 0.6 ㎛, respectively at -1.6 V, and 5.3 ㎛ and 1.8 ㎛, respectively at -1.8 V. In the low potential range, the effect of molecular hydrogen was greater than that of atomic hydrogen, and much hydrogen gases were generated running the experiment. In the case of 3,600 seconds of experiment time, severe corrosion and rough surface morphologies were observed at -0.5 V due to high current density resulting from active dissolution reaction, and the 3D analysis found that the maximum damage depth and the mean damage depth were 5.1 ㎛ and 2.2 ㎛, respectively. At -0.8 V which corresponded to the corrosion resistance section on the current density comparison curve, a clean surface with almost no corrosion was observed. The maximum damage depth and the mean damage depth were 0.7 ㎛ and 0.4 ㎛, respectively, and there was no damage by corrosion. At -1.6 V which corresponds to the activation polarization section, the maximum damage depth and the mean damage depth at the center of specimens were high at 6.4 ㎛ and 4.4 ㎛, respectively, due to the effect of molecular hydrogen. At the potential of -1.8 V, on the other hand, a high current density was observed due to excessive activation reaction, and the damages became severer due to the activation polarization resulting from the generation of hydrogen gas as the potential moved to the active direction. The maximum damage depth and the mean damage depth were 7.7 ㎛ and 3.2 ㎛, respectively. The effect of molecular hydrogen was dominant and the damages could be observed with naked eyes. Similar trends were observed for the variable of potentiostatic experiment time. The damage depth tended to be deeper outside the corrosion resistance section and also when the application time was longer.

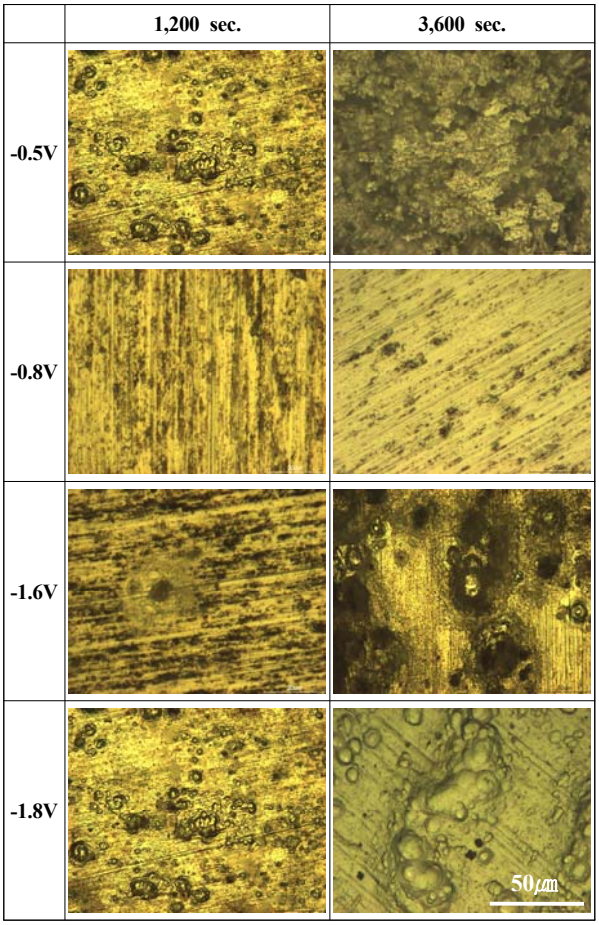

Figure 7: Surface morphologies after potentiostatic experiment during 1,200 sec. and 3,600 sec. for 5083-H116 alloy

4. Conclusions

The maximum damage depth and the mean damage depth were analyzed for each applied potential through 3D analysis after potentiostatic experiment at different rotation speed, and it was found that the higher the rotation speed was, the greater the damage depth became. As the difference in damages was very small at -0.9 V and -1.2 V which corresponded to the corrosion resistance section, almost no difference by the existence of flow was observed. The correlation between the maximum and mean damage depths and the current density was examined, and the smallest damages occurred in the corrosion resistance section. As a result of comparing the current density and the degree of damages after the potentiostatic experiment for 1,200 and 3,600 seconds, the section from -1.25 to -0.75 V and the section from -1.2 to -0.8 V corresponded to the corrosion resistance sections. Thus, the common section from -1.2 to -0.8 V appears to be the optimum corrosion resistance section.

Acknowledgement

This research was financially supported by the Ministry of Education (MOE) and National Research Foundation of Korea (NRF) through the Human Resource Training Project for Regional Innovation (No. 2011-09-U-01-039).

References

[1] Sky Al Products Corporation, “Foundation of Al alloy ship projects,” Light Metal Welding of Japan, vol. 41, no. 11, pp. 544-545, 2003.

[2] S. J. Kim and S. K. Jang, “Mechanical and electrochemical characteristics in welding with robot on 6061-T6 Al alloy for Al ship,” Journal of the Korean Society of Marine Engineering, vol. 33, no. 2, pp. 313-321, 2009.

[3] S. J. Kim, “The material and welding technology for Al ship,” Journal of the Korean Society of Marine Engineering, vol. 30, no. 5, pp. 540-551, 2006.

[4] S. K. Jang and S. J. Kim, “Mechanical and electrochemical characteristics of welding parts surface for friction Stir welded 5456-H116 Al alloy,” Journal of the Korean Institute of Surface Engineering, vol. 41, no. 4, pp. 156-162, 2008.

[5] K. G. Kerschbaumer, R. Vallant, N. Enzinger, and C. Sommitsch, “Welded aluminium and magnesium alloys - corrosion and mechanical properties for refrigeration compressors in comparison with deep-drawing steel,” Materiali in Tehnologije, vol. 47, no. 3, pp. 363-377, 2013.

[6] C. Vargel, Corrosion of Aluminium, 1st Edition, Elsevier, London, p. 101, 2004.

[7] S. J. Kim, J. Y. Ko, and M. S. Han, “Evaluation of the characteristics using slow strain rate tests of 5456 Al-Mg alloy for ship construction,” The Korean Journal of Chemical Engineering, vol. 23, no. 6, pp. 1028-1033, 2006.

[8] D. H. Kim, S. J. Kim, K. M. Moon, M. H. Lee, and K. J. Kim, “Influence on consumption rate and performance of aluminum sacrificial anode due to seawater velocity and pH variations,” Journal of the Corrosion Science Society of Korea, vol. 30, no. 1, pp. 1-10, 2001.